A SARS–CoV-2 Spike Receptor Binding Motif Peptide Induces Anti-Spike Antibodies in Mice andIs Recognized by COVID-19 Patients

Federico Pratesi, Fosca Errante, Lorenzo Pacini, Irina Charlot Peña-Moreno, Sebastian Quiceno, Alfonso Carotenuto, Saidou Balam, Drissa Konaté, Mahamadou Diakité, Anna Papini, et al.

A SARS–CoV-2 Spike Receptor Binding Motif peptide induces anti-spike antibodies in mice and is recognized by COVID-19 patients

Federico Pratesi[1*], Fosca Errante[2*], Lorenzo Pacini[3*], Irina Charlot Peña-Moreno[4], Sebastian Quiceno[4], Alfonso Carotenuto[5], Saidou Balam [6,7], Drissa Konaté[6], Mahamadou M Diakité[6], Anna M. Papini[3], Myriam Arévalo-Herrera[8,] Paola Migliorini[1], Andrey V. Kajava[9], Paolo Rovero[2], Giampietro Corradin[10], Sócrates Herrera[4].

[1] Department of Clinical and Experimental Medicine, University Hospital of Pisa, Pisa, Italy

[2] Interdepartmental Laboratory of Peptide and Protein Chemistry and Biology, Department of NeuroFarBa, University of Florence, Sesto Fiorentino, Italy

[3] Interdepartmental Laboratory of Peptide and Protein Chemistry and Biology, Department of Chemistry "Ugo Schiff", University of Florence, Sesto Fiorentino, Italy

[4] Caucaseco Scientific Research Center, Cali, Colombia

[5]Department of Pharmacy, University of Naples Federico II, via D. Montesano 49, 80131 Naples, Italy

[6] Immunogenetic Laboratory and Parasitology, University of sciences, techniques and technologies of Bamako (USTTB), Mali

[7] Department of Nephrology, University Hospital Regensburg, Regensburg

[8]Malaria Vaccine Development Center, Cali, Colombia

[9] CRBM, University of Montpellier, CNRS, Montpellier, France

[10]University of Lausanne, Lausanne, Switzerland

*Contributed equally to this work

Corresponding author:
Sócrates Herrera, sherrera@inmuno.org
Phone: (+57) 317 517 0552
Caucaseco Scientific Research Center
Cali, Colombia

Abstract

The currently devastating pandemic of severe acute respiratory syndrome known as coronavirus disease 2019 or COVID-19 is caused by the coronavirus SARS-CoV-2. Both the virus and the disease have been extensively studied worldwide. A trimeric spike (S) protein expressed on the virus outer bilayer leaflet has been identified as a ligand that allows the virus to penetrate human host cells and cause infection. Its receptor-binding domain (RBD) interacts with the angiotensin-converting enzyme 2 (ACE2), the host-cell viral receptor, and is, therefore, the subject of intense research for the development of virus control means, particularly vaccines. In this work, we search for smaller fragments of the S protein able to elicit virus-neutralizing antibodies, suitable for production by peptide synthesis technology. Based on the analysis of available data, we selected a 72 aa long receptor binding motif ($RBM_{436-507}$) of RBD. We used ELISA to analyze the antibody response to each of the three antigens (S protein, its RBD domain and the $RBM_{436-507}$ peptide) in humans exposed to the infection and in immunized mice. The seroreactivity of these three antigens and the antibody role in virus neutralization were determined. These results provide a basis for further studies towards the development of vaccines or treatments focused on specific regions of the S virus protein, which can benefit from the absence of folding problems, conformational constraints and other advantages of the peptide synthesis production.

Introduction

The current SARS-CoV-2 (severe acute respiratory syndrome coronavirus 2) pandemic has resulted in devastating social and economic consequences worldwide, in addition to an enormous public health burden. Coronaviruses are single-stranded RNA-enveloped viruses [1]. Although this type of viruses is frequently associated with a common cold with mild symptoms in humans, some of them can cause severe respiratory infection and death, mainly in elderly patients and in individuals with several comorbidities, primarily diabetes, obesity, hypertension and other cardiovascular disorders [2-4].

The ongoing coronavirus disease 2019 (COVID-19) is considered one of the world's worst pandemics, with more than 200 million cases and 4 million human deaths reported by January 2021 [5]. Since the beginning of the COVID-19 pandemic, the scientific community has focused intense efforts on studying the virus biology, the disease manifestations and management and its prevention [6-8]. In a short time, the SARS-CoV-2 genome, the specificity of its overall structural organization and the atomic 3D structure of the most significant proteins were revealed [9, 10].

One of the critical proteins is a trimeric spike (S) protein that allows this virus to penetrate host cells and cause infection. The S protein trimers protrude from the outer bilayer leaflet and form a characteristic crown-like halo surrounding the viral particle (hence, "corona"). The importance of the SARS-CoV2 S-protein is that it is a large self-assembled homo-trimer protein of about 1,250 aa [9, 12, 34], expressed on the virus membrane and responsible for the virus-cell invasion. The protein is composed of two functional subunits, S1 and S2. The S1 subunit, which forms the globular head of the S protein trimer, contains the receptor-binding domain (RBD) that specifically interacts with the host receptor angiotensin-converting enzyme 2 (ACE2).

The S2 subunits form the stalk of the trimer embedded into the viral envelope. When the S protein binds to the ACE2 receptor, proteases located on the host cell membrane trigger the dissociation of S1 fragments and induce an irreversible refolding of the S2 trimer. The structural

rearrangement of S2 brings together the viral and cellular membranes, leading to the fusion of the two bilayers. The atomic 3D structure of the S trimer in the prefusion conformation, the S2 trimer in the post-fusion conformation, and the RBD-ACE2 complex have been determined [10-15] and all have contributed to developing means to control virus spreading. Specifically, these features of the S protein led vaccine companies, i.e., Pfizer and Moderna [35, 36] to choose it for vaccine development.

The RBD is a monomeric domain of a smaller size (220 aa) that folds in the same stable 3D structure as part of the complete S protein and as a separate domain [37]. Antiviral antibodies and cell mediated responses of multiple specificities are produced during SARS-CoV-2 infection and appear to contribute to protection [11]. RBD is not only essential for virus invasion of host cells, but also targets neutralizing antibodies generated during SARS-CoV-2 infection; therefore, RBD represents another promising vaccine candidate [6, 38, 39]

While the rate of infections and deaths rapidly increased worldwide, significant efforts were invested in developing effective tools to promptly confirm diagnosis of the infection i.e., highly sensitive and specific molecular diagnostic methods [15]. Likewise, given that vaccines are the primary medical option and most cost-effective means for global control of the pandemic, an unprecedented effort to develop anti-COVID-19 vaccines led to the production, clinical evaluation and approval by regulatory agencies of multiple vaccines. Along this line, given the critical functions of the S protein, the viral surface location, and the availability of detailed structural information, this protein was chosen for vaccine development [9, 16-19].

As of January 2022, more than nine billion vaccine doses had been delivered globally, and ~60% of the world population had received at least one vaccine dose [5]. Moreover, despite specific antiviral drugs having been elusive until recently, two novel antiviral medicines have already been approved by the United States Food and Drug Administration (FDA). Molnupiravir produced by Merck [20], and Nirmatrelvir/Ritonavir (Paxlovid) produced by Pfizer [21] are medicines for oral administration, with high effectiveness to reduce disease severity and prevent deaths [22].

Although the most extensively used vaccines have shown high protective efficacy, their effectivity, particularly the antibody response's longevity and the virus-neutralizing function, appears short-lasting, suggesting the need for new vaccine formulations. Based on the recent advances in understanding the structure and function of S protein, and with the aim of identifying highly effective virus proteins/fragments this work focused on further characterization of the S protein, focusing on shorter fragments/domains with vaccine potential. We selected the S-ACE2 receptor binding motif ($RBM_{436-507}$) which was produced as a single synthetic peptide, along with shorter sequences which were compared in their antigenicity and immunogenicity using sera from humans naturally exposed to or vaccinated against COVID-19, and sera from immunized animals. Selected sera were also analyzed for their neutralization activity.

Materials and Methods

Recombinant S and RBD proteins production

Since the S trimer is described as the primary protein responsible for inducing a protective immune response against the SARS-CoV-2 virus, first we produced a secreted and soluble form of this protein self-assembled in the trimer using Chinese Hamster Ovary (CHO) cells as previously described [23]. Briefly, the transmembrane domain and the C terminal intracellular tail were removed and replaced by a T4 foldon DNA sequence [24] and a 8xHis tag. A signal peptide sequence was added. To stabilize the prefusion structure of the S trimer in our constructs, we deactivated the original RRA furin cleavage site R by changing it to RGSA. We introduced amino-acid mutations K986P/V987P ("2P") as suggested elsewhere [14]. The construct used in this work had the D614G mutation shared by most of the SARS-CoV-2 Variant of concern (B.1.1.7 – Alpha, B.1.351 – Beta, B.1.617.2 – Delta, B.1.1.529 Omicron) widely spread in Europe during the 2020-2021 pandemic [25]. This S protein construct was established to form trimers predominantly folded in the prefusion conformation [26]. In addition, the RBD of the S protein (aa 319-541) was produced as a recombinant product [26] and a series of peptides covering the BIP sequence were synthesized and analyzed.

Peptide synthesis, purification and characterization

Peptide sequences corresponding to the full $RBM_{436-507}$ length (72 aa) as well as shorter fragments of 20-22 amino acids (P11-P16) described in **Table 1** were synthesized and analyzed. Single cysteine residues in peptides P11, P12, and P13 (486-507, 476-495 and 466-485 of S protein, respectively) were replaced with serine to avoid unwanted spontaneous formation of disulfide dimers. Peptides were prepared by microwave-assisted solid-phase peptide synthesis (MW-SPPS), cleaved from the resin and, in the case of $RBM_{436-507}$ and P12, oxidized in solution with H_2O_2 at pH 9.0. Purifications were performed by flash chromatography followed by semi-preparative HPLC to achieve purity >70% ($RBM_{436-507}$ and P16) or >87% (P11-P15). Final products were characterized by analytical UHPLC coupled with ESI single quadrupole mass spectrometry and/or MALDI-ToF analysis. Analytical data and details on the synthesis and purification procedures are available as Supplementary Information.

Conformational studies by circular dichroism

The CD spectrum of the $RBM_{436-507}$ peptide was recorded using quartz cells of 0.1 cm path length with a JASCO J-710 CD spectropolarimeter at 25 °C. The spectrum was measured in the 260−190 nm spectral range, 1 nm bandwidth, 64 accumulations, and 100 nm/min scanning speed. The peptide was dissolved in water to a concentration of 12 μM. The secondary structure content of the peptide was predicted using the online server for protein secondary structure analyses DichroWeb [27]. Input and output units and the wavelength step were θ (mdeg) and 1.0 nm, respectively. The algorithm used was CDSSTR, and the reference database was set-7 [23]**.** The normalized root means square deviation (NRMSD) was 0.035.

Human blood samples

A clinical protocol was developed, submitted to and approved by the local Ethical Committees (CEAVNO, Approval # 17522) in Italy and (CECIV, approval # 04-2020) in Colombia. Whole blood (10 mL) was collected from COVID-19 patients and vaccinated volunteers from both Italy and Colombia. Samples were collected by arm venipuncture using dry tubes after hospitalization, and upon the patient's written informed consent, socio-demographic data and clinical manifestations

were recorded. SARS-CoV-2 infection was confirmed by RT-PCR. Blood was fractionated, and sera were collected and kept frozen at -20^{o}C until use for serology.

Mice immunization and sera collection

A total of 30 male and female, 6-8 weeks old BALB/c mice of 20 ± 5 g of body weight were randomly selected and distributed in three groups (A, B and C) of 10 animals each. Each group was further divided into experimental (Exp) and control (Ctrl) sub-groups of five mice each and were further immunized with SARS-CoV-19 recombinant S (group A), recombinant RDB (group B) protein as well as with the synthetic $RBM_{436-507}$ peptide (group C). Each group of mice was immunized subcutaneously (s.c.) at the base of the tail on days 0, 20 and 40 with 20 μg of each antigen diluted in 50 μL PBS and emulsified in Montanide ISA-51 (Seppic Inc., Paris, France) according to the manufacturer's recommendations. Mice were bled from submandibular veins on days 1-2 before the first and third immunizations, 20 days after the third dose and every 60 days until day 140. Whole blood (~100 μL) was collected, and sera were separated by centrifugation and stored frozen at -20°C until use for serological analyses. Animal studies were carried out at the Caucaseco Research Center in Cali (Colombia) and approved by the Animal Ethics Committee of MVDC in Colombia. Animal care, housing, and handling were performed according to institutional guidelines and following the National Institutes of Health Guide for the Care and Use of Laboratory Animals.

Serological analyses

Reactivity of mouse antibodies to S and RBD proteins and $RBM_{436-507}$

The reactivity of sera from mice immunized with the S, RBD and $RBM_{436-507}$ was determined by ELISA, using as antigens the specific immunogens. Briefly, 96-well plates (Nunc-Immuno Plate, Maxisorp, Roskilde, Denmark) were coated with one μg/mL $RBM_{436-507}$, RBD and Spike Trimer protein, pH 7.4 at 4°C, overnight. After plates were blocked with 5% skim milk solution [PBS 1X, 0.05% Tween 20, (PBS-T)], serum samples were added at 1:100 or three-fold serial dilutions starting at 1:100 in 2.5% skim milk in PBS-T and were incubated for 1 hour. Plates were then washed and incubated with alkaline phosphatase-conjugated anti-mouse IgG antibody (Sigma

Chemical Co., St Louis, MO) at a 1:1000 dilution for 1 hour. Reactions were revealed with para-nitrophenyl phosphate substrate (*p*-NPP) (Sigma Aldrich) and read at 405 nm wavelength (Dynex Technologies, Inc., MRX Chantilly, VA).

ELISA assays to analyze anti-Spike, anti-RBD and anti-RBM$_{436-507}$ human antibodies

Nunc Maxisorp polystyrene plates were coated with Spike Trimer (Excellgene, Monthey, Switzerland) or RBD (Excellgene, Monthey, Switzerland) at 1 μg/ml in PBS pH 7.4 (50 μl/well) overnight at 4°C; peptide RBM$_{436-507}$ coating was at 2 μg/ml in Carbonate buffer, pH 9.6; 20-mers P11-P16 at 10 μg/ml in PBS, pH 7.4. After blocking for 1 hr at room temperature (RT) with PBS pH 7.4, BSA 3% (A4503 - Merck KGaA, Darmstadt, Germany), sera diluted 1/100 in PBS pH 7.4, BSA 1%, Tween-20 0.05% were incubated on the plate (50 μl/well) for 2 hours at RT. After 3 washings with PBS Tween-20 0.05% (150 μl/well), goat anti-human IgG HRP (A0293 - Merck) diluted 1:5000 in PBS BSA 1% Tween-20 0.05% was added to the plates at 50 μl/well and incubated for 2 hours. For IgM and IgA determination, goat anti-human IgM HRP conjugate (A0420 – Merck) or goat anti-human IgA HRP conjugate (A0295 - Merck) diluted 1:20,000 in PBS, BSA 1%, Tween 0.05% were added to the plates. After three washings with PBS Tween-20, 0.05%, enzymatic activity was measured at 450 nm after TMB addition (T4444 - Merck) and blocked by H_2SO_4 1M.

Inhibition of ACE binding to RBD with anti-RBM$_{436-507}$ specific human antibodies

The ability of anti-RBM$_{436-507}$ antibodies to inhibit the binding of ACE2 to RBD was evaluated using a modification of the SPIA commercial kit (Diametra Srl, Spello, Pg - Italy, ImmunoDiagnostic System Group). Anti-RBD antibodies were used as a positive control. Anti-N1 (20-mer linear peptide of SARS-CoV-2 nucleocapsid, aa 366-388) and anti-TT (tetanus toxoid) antibodies were used as virus-related and -unrelated negative controls. Specific antibodies were eluted from four sera with high anti-COVID-19 antibody titers using polystyrene plates coated with RBD, RBM$_{436-507}$, N1 and TT. Briefly, the plates were blocked with PBS BSA 3%, and COVID-19 sera diluted 1/50 in PBS BSA 1% Tween-20 0.05%, and incubated for 2 hours at RT. Plates were washed three times with PBS Tween-20 0.05%, and bound antibodies were eluted with 200 μl PBS pH 3.0 and

immediately neutralized at pH 7.4 with basic phosphate buffer. The concentration of eluted antibodies was evaluated by A_{280} absorbance measurement with Nanodrop, and binding to the respective antigen was confirmed by indirect ELISA. For ACE inhibition assay, anti-RBD, anti-$RBM_{436-507}$, anti-N1 and anti-TT eluted antibodies were incubated onto Diametra SPIA plates coated with recombinant RBD. Calibrator and controls were loaded as per the manufacturer's instructions. Ready-to-use ACE2 conjugated with horseradish peroxidase was then added to the wells, and plates were incubated for 90 minutes at 37°C. After washings, plates were incubated with TMB for 15 minutes and acid stop solution was added before reading the absorbance at 450 nm. Results were expressed as percentage inhibition according to the manufacturer's instruction.

Statistical analysis

Antibody titers were compared between mouse groups. A descriptive analysis was performed to evaluate differences in humoral immune responses within each group of mice. Kruskal-Wallis was performed to compare the antibody response to each protein, followed by Dunn's multiple comparison test. Results of anti-S, anti-RBD and anti- $RBM_{436-507}$ antibodies were expressed as Odd Ratio (OR) of a positive internal control set at 1.0. A p-value < 0.05 was considered statistically significant. Data were analyzed and plotted using GraphPad Prism software (version 5.01; GraphPad Software Inc, San Diego, California, USA).

Results

Selection and circular dichroism analysis of $RBM_{436-507}$ peptide

To study the interaction between S and ACE2, we focused on the surface of the RBD involved in the ACE2 receptor binding, which should represent the target of the neutralizing antibodies. Our analysis of the 3D structure of the RBD-ACE2 complex showed that the large part of the RBD interacting surface, the Receptor Binding Motif (RBM), is composed of a 436-507 aa segment (**Figures. 1A-C**). Since peptide synthesis technology has several advantages compared to recombinant proteins [24, 28], we selected this RBM region for peptide synthesis and subsequent experimental studies. The central part of $RBM_{436-507}$ should mimic well the native-like conformation due to a disulfide bond. The peptide flanking parts should be unstructured and

highly flexible both in peptides as well as within the 3D structure of the S-protein. In addition to the critical surface localization of the $RBM_{436-507}$ in the S protein, its amino acid sequence is specific to the SARS-CoV-2 and contains several predicted T-cell epitopes [29]. The sequence of $RBM_{436-507}$ (**Table 1**) was N-terminal acetylated and C-terminal amidated to avoid including terminal charged groups not present in the native protein.

The conformation of $RBM_{436-507}$ in water at pH 7 was explored by CD spectrometry (**Figure 1D**). We then evaluated the antigenic properties of this peptide. The absence of a defined minimum around 200 nm, diagnostic of random coil conformation, is compatible with a certain degree of structuration of the peptide. The secondary structure content was predicted based on the CD spectrum using the online server for protein secondary structure analyses, DichroWeb [22]: 2% helix, 30% β-strand, 19% β-turn, and 49% random coil. The relatively high percentage of β-strand conformation suggests the intriguing hypothesis that $RBM_{436-507}$ peptide can partially preserve the extended conformation displayed along most of its sequence within the folded Spike protein (pdb code 6VXX) [16, 27].

Immunogenicity of S, RBD and $RBM_{436-507}$ in mice

As shown in **Figure 2**, sera from all immunized animals tested by ELISA at 1:100 dilution, in response to the S, RBD and $RBM_{436-507}$ antigens, indicated specific IgG seroconversion after the first immunization dose. Furthermore, most of them displayed a boosting response after the second immunization dose, with the highest levels against the three proteins observed on day 40. However, while animals immunized with $RBM_{436-507}$ and RBD developed similar high level antibody profiles (3.0 to 3.5 OD), mice immunized with the S protein displayed significantly lower responses (1.0 to 2.0 OD). For $RBM_{436-507}$ and RBD, antibodies remained at high levels (>2.0 OD) after day 140, whereas antibodies against the S protein notably decreased ($\leq$ 0.5 0D) during the same period. None of the control mice immunized with adjuvant alone seroconverted. The antibody titration (three-fold dilutions) using sera collected on day 140 indicated titers of 1:24,300, 1:72,900 to $RBM_{436-507}$ and RBD respectively, and 1:900 to S (Supplemental Material, **Figure S1a**).

287

288 **Reactivity of mouse antibodies to S, RBD and $RBM_{436-507}$**

289 The analysis of the homologous and cross recognition of the S, RBD and $RBM_{436-507}$ antigens by
290 antibodies elicited upon mice immunization is shown in **Figure 3**. ELISA results showed a high
291 homologous sera reactivity but different reactivity with the other proteins/domains. Reactivity
292 of sera diluted at 1:100 showed OD values ranging from 1.2 to 2.0 against the full-length S
293 antigen, 3.2-3.5 to the RBD and 3.0-3-5 to the $RBM_{436-507}$ fragment. The titration of this
294 homologous reactivity indicated that final reactivity (OD 0,2) at $1:10^4$ dilution to the S protein
295 (**Figure 3** upper panel), whereas at the final dilution tested ($1:10^4$) the OD values were
296 significantly higher for RBD (OD= 2.5-3.0) and RBM (0.5-1.7) **(Figures 3B and 3C**, respectively).
297 Regarding the analysis of the cross reactivity, anti-S antibodies displayed similar recognition of
298 RBD and $RBM_{436-507}$ (**Figure 3A**), and the anti-RBD antibodies high recognition of both the S- and
299 -$RBM_{436-507}$ proteins, although the S-protein was better recognized (p=xx). In contrast, for the
300 anti-$RBM_{436-507}$ antibodies, only two mice presented cross reactivity with end point of $1:10^4$
301 whereas the remaining animals of the group presented only weak reactivity at 1:100 dilution.
302 Notably, these antibodies did not cross react with the S-protein.
303

304 The final reactivity titer of the anti-S antibodies was $1:10^4$ against the S protein, and $1.8x10^3$
305 against RBD and $RBM_{436-507}$. In the case of RBD, mouse immunization elicited a vigorous antibody
306 response **(Figure 3B)** with high optical densities even at $1:10^4$ dilution. Although reactivity to the
307 S protein and the $RBM_{436-507}$ peptide were lower, recognition remained significant even at
308 dilutions of $1:10^4$ and $5:10^3$, respectively. Sera from mice immunized with $RBM_{436-507}$ peptide also
309 displayed high reactivity with the homologous peptide and the RBD protein; however, these sera
310 did not react with the S protein **(Figure 3C).** We further analyzed reactivity of anti-$RBM_{436-507}$
311 antibodies upon solid-phase capture on ELISA plates followed by glycine elution with its
312 homologous peptide, the RBD and the S proteins. As shown in **Figure 4**, while there was
313 significant reactivity of eluted antibodies with $RBM_{436-507}$, no recognition of the motif on the RBD
314 and S proteins was observed.
315

316 **Evaluation of anti- RBM$_{436-507}$ antibodies in humans**

317 Patient sera were first screened by ELISA using S and RBD proteins and compared to a group of
318 pre-pandemic normal sera. IgG antibody levels higher than the 97.5th percentile of normal sera
319 were detected in 45% (29/64) of patient sera on S and in 53% (34/64) on RBD (**Figure 5A and 5B**).
320 A strong positive correlation (p<0,0001) was observed between antibody levels for the two
321 recombinant proteins (**Figure 5C**).

322

323 It has been shown that low pH affects spike structure, favoring a closed conformation of the
324 trimer [30], affecting epitope exposure [13]. We thus performed the ELISA assay at acidic pH,
325 obtaining a similar level of antibodies in patient sera (Supplementary Figures 2a and 2b). Sera
326 from COVID-19 patients and normal subjects were tested by ELISA using RBM immobilized on
327 polystyrene plates (see Materials and Methods for details). IgG anti-RBM$_{436-507}$ higher than the
328 97.5th percentile of the average population was detected in 21/60 (35%) of the COVID-19
329 patients. IgG antibody levels were significantly higher in patients than in controls (p<0.05) (**Figure**
330 **6A**) and were correlated with anti-Spike and anti-RBD antibody levels (p < 0.01) (**Figures 6D and**
331 **6E**). Anti RBM$_{436-507}$ of IgM and IgA isotype were also evaluated, with IgM anti- RBM$_{436-507}$
332 detected in 7/60 (11.6%) and IgA in 6/60 (10%) (**Figures 6B and 6C**). IgM and IgA antibody levels
333 were not significantly different in COVID-19 patients and controls. There was coexpression of
334 anti- RBM$_{436-507}$ Ig isotypes in COVID-19 samples (**Figure 6F**).

335

336 **Epitope mapping and functional activity of murine and human anti-RBM$_{436-507}$ antibodies**

337 The analysis of the neutralizing activity of antibodies elicited by mouse immunization showed
338 that, for mice immunized with S and RBD on days 0, 20 and 40, the percentage of neutralization
339 increased with the priming dose and was significantly boosted after the second and third doses.
340 Both S and RBD sera induced total neutralization after the third dose and remained high until the
341 last test on day 115. In contrast, antibodies to RBM$_{436-507}$ reached 40% neutralization, which
342 remained at that level until day 115 (**Figure 7)**. The analysis of the cross neutralization of sera of
343 the three groups of animals immunized with S, RBD and RBM$_{436-507}$.

344

To determine whether $RBM_{436-507}$ represents a target of neutralizing antibodies in natural conditions, we first carried out an extensive ELISA analysis of sera from both COVID-19 patients and immunized mice. In the case of human sera (n= 100) from COVID patients 35 (35%) reacted with the $RBM_{436-507}$ indicating a lower reactivity than the same sera with the S and RBD. Positive samples displayed distinct reactivity with different regions of $RBM_{436-507}$, more frequently with the N-terminal portion (P15-P16).

Neutralizing activity of anti-$RBM_{436-507}$ antibodies has been evaluated by inhibition of RBD binding to ACE2, an assay considered a SARS-CoV-2 surrogate virus neutralization test [31-33]. Neutralizing antibodies may bind to sequences exposed both in the closed and the open conformation of the S protein or only in the open one; most of these sequences are comprised in $RBM_{436-507}$. In contrast, mice immunized with $RBM_{436-507}$ presented good recognition of $RBM_{436-507}$ and RBD but no reactivity with S.

Second, because neutralizing antibodies mostly specific for RBD but also to several targeted epitopes are produced during natural infection [17], we compared the ACE2-RBD binding neutralization by antibodies to the whole RBD and to $RBM_{436-507}$. **Figure 9** shows that in the case of humans with confirmed COVID-19 infection, sera positive to $RBM_{436-507}$ were tested using the 20-mer overlapping peptides covering the entire RBM sequence (Table 1). As shown in **Figure 8**, immune response mainly targets the N terminal domain (P15-P16) rather than the C-terminal part (P11-P12). To evaluate the ability of antibodies to RBD or $RBM_{436-507}$ sequences to block ACE2 binding to RBD, specific anti-RBD and anti-$RBM_{436-507}$ antibodies were eluted from COVID-19 positive sera using antigen-coated wells and incubated with labeled ACE2 on solid-phase RBD. Anti-RBD antibodies eluted from 4 COVID-19 sera inhibited the binding of labeled ACE2 to solid-phase RBD (**Figures 6B and 6C**). Anti- $RBM_{436-507}$ antibodies from 2 out of 4 sera displayed some inhibition, higher than anti-N1 and anti-TT control antibodies.

Discussion

This study confirmed the high seroreactivity and immunogenicity of the full-length S and RBD recombinant proteins and the synthetic $RBM_{436-507}$ fragment. More importantly, it compared the antibody responses induced by natural human exposure to SARS-CoV2 and vaccination with that of rodents experimentally immunized with the three antigens.

Analysis of 3D structures of the S protein and RBD-ACE2 complex led to selecting a RBD 72 aa long segment ($RBM_{436-507}$) highly specific to SARS-CoV-2 and located in the RBD-ACE2 interface. Importantly, *in silico* studies confirmed the presence in this protein fragment of multiple immune epitopes (B- and T-cell epitopes) previously identified [29], and our CD data suggested that the $RBM_{436-507}$ peptide alone can partially preserve the extended beta-conformation observed in the context of the native protein structure.

These features, together with the high RBD immunogenicity during human natural infection, vaccination and animal immunization, as well as the efficient neutralization of the RBD-ACE2 interaction by anti-RBD antibodies, encouraged the search for a smaller fragment with vaccine potential, suitable for production by peptide synthesis technology. It was hoped that the smaller fragment could elicit virus-neutralizing antibodies with similar or superior vaccine performance than the S protein.

The multiple vaccines delivered worldwide are based on the full-length S protein using different technological platforms [40, 41]. Although most of them have displayed high protective efficacy, their effectivity, particularly the antibody response's longevity and the virus-neutralizing function, appears short-lasting. Within less than a year of a two doses immunization schedule, a third vaccine dose was required to maintain the protection level; moreover, boosting vaccine doses may be further required to offer functional immunity in the population [42]. Because of the vast virus propagation capacity in the population, frequent vaccination generates a significant logistic and global economic challenge; therefore, alternative vaccine platforms are envisioned.

The strong positive correlation of the ELISA seroreactivity of the S (45% = 29/64) and RBD (53% = 34/64) proteins ($p<0,0001$) is very interesting and confirms the feasibility of using a fragment of the S protein as vaccine. In addition, this result correlates with the highly efficient neutralization induced by mouse anti-S and -RBD sera. Moreover, the IgG ELISA reactivity of these two proteins with COVID19 and pre-pandemic normal sera (>97.5th percentile) indirectly confirmed the response specificity to SARS-COV-2. In contrast, specific IgM and IgA antibody levels were similar in COVID-19 patients and controls (**Figure 6F)**. This latter finding may be explained because control sera never had anti- SARS-CoV2 antibodies and in the COVID-19 sera the primary IgM response and IgA had waned. These results support the idea that shorter protein fragments i.e. RBD would have the capacity to stimulate at least a similar immune response to S protein.

We show here that the antibody recognition of $RBM_{436-507}$ as an isolated fragment, i.e., as $RBM_{436-507}$ peptide, was limited to only a fraction of COVID-19 donors. In COVID-19 patients, a polyclonal anti-$RBM_{436-507}$ antibody response with IgM, IgG and IgA isotypes was detected in one third of the cases, in amounts correlated with the level of anti-RBD and anti-S antibodies.

Our finding that $RBM_{436-507}$ and smaller peptides is in agreement with a report from 2020 [18] showing that COVID-19 patients produced antibodies to multiple sequences, such as S412-431 and S446-465, that overlap ACE2 contact residues, and S432-451 and S475-494, that are adjacent to critical residues contacted by ACE2, all contained within $RBM_{436-507}$.

The high level of neutralization achieved by mice sera after the first immunization dose with RBM?? encouraged selection of a smaller protein fragment with vaccine potential (**Figure 7)**. Complete neutralization is produced after the first immunization with RBD, whereas similar neutralization by anti-S antibodies is only obtained after two immunization doses. In contrast, the poor neutralization of the anti-$RBM_{436-507}$ antibodies was unexpected and deserves further studies. This result is surprising as there was significant cross reactivity of anti-RBD and anti-$RBM_{436-507}$ (**Figure 3**).

The neutralizing activity of anti-$RBM_{436-507}$ antibodies might be associated with the lack of recognition of the full-length S by the anti-$RBM_{436-507}$ sera. In addition, the high immunogenicity of $RBM_{436-507}$ mice confirms the presence of T-cell epitopes within this protein segment, as suggested by the analysis performed by Grifoni et al. [29].

Mouse, humans IgG antibodies efficiently reacted with both $RBM_{436-507}$ and RBD, but not with S. The latter results can be explained by the fact that $RBM_{436-507}$ represent only 6-7% of the whole protein. Moreover, anti-$RBM_{436-507}$ specific antibodies elicited by mice immunization only partially inhibited (30-40%) the RBD-ACE2 interaction, while mouse anti S and RBD recognized RBM and induced 100% inhibition of the ligand-receptor interaction. These results suggest that the conformation of isolated $RBM_{436-507}$ only partially overlaps with the RBM structures present in S or RDB. The relatively high percentage of β-strand conformation suggests that $RBM_{436-507}$ peptide alone can partially preserve the extended conformation displayed along most of its sequence within the folded S protein (pdb code 6VXX) [17, 19].

In conclusion, our comparative analysis of immunological properties has shown that although $RBM_{436-507}$ had reduced seroreactivity compared to the S protein and RBD, it could still be an alternative path for developing virus control means, particularly vaccines. The basis for this potential lies in its small size, absence of folding problems, possibility to constraint the RBM conformation in a required state, easy incorporation in different multimeric carriers and advantages associated with peptide synthesis production.

Acknweledgment

References

1. Fehr, A.R. and S. Perlman, *Coronaviruses: an overview of their replication and pathogenesis.* Methods Mol Biol, 2015. **1282**: p. 1-23.
2. Matsuyama, R., et al., *Clinical determinants of the severity of Middle East respiratory syndrome (MERS): a systematic review and meta-analysis.* BMC Public Health, 2016. **16**(1): p. 1203.
3. O'Driscoll, M., et al., *Age-specific mortality and immunity patterns of SARS-CoV-2.* Nature, 2021. **590**(7844): p. 140-145.
4. Williamson, E.J., et al., *Factors associated with COVID-19-related death using OpenSAFELY.* Nature, 2020. **584**(7821): p. 430-436.
5. WHO. *Weekly epidemiological update on COVID-19* 2022 [cited 2022; 78:[
6. Yuan, Y., et al., *A bivalent nanoparticle vaccine exhibits potent cross-protection against the variants of SARS-CoV-2.* Cell Rep, 2022. **38**(3): p. 110256.
7. Li, C.X., et al., *A critical analysis of SARS-CoV-2 (COVID-19) complexities, emerging variants, and therapeutic interventions and vaccination strategies.* Biomed Pharmacother, 2022. **146**: p. 112550.
8. Baghban, R. and S. Mahmoodi, *Nucleic Acid-Based Vaccines Platform Against Covid-19 Pandemic.* Curr Mol Med, 2022.
9. Ismail, A.M. and A.A. Elfiky, *SARS-CoV-2 spike behavior in situ: a Cryo-EM images for a better understanding of the COVID-19 pandemic.* Signal Transduct Target Ther, 2020. **5**(1): p. 252.
10. Wierbowski, S.D., et al., *A 3D structural SARS-CoV-2-human interactome to explore genetic and drug perturbations.* Nat Methods, 2021. **18**(12): p. 1477-1488.
11. Fan, X., et al., *Cryo-EM analysis of the post-fusion structure of the SARS-CoV spike glycoprotein.* Nat Commun, 2020. **11**(1): p. 3618.
12. Cai, Y., et al., *Distinct conformational states of SARS-CoV-2 spike protein.* Science, 2020. **369**(6511): p. 1586-1592.
13. Tortorici, M.A., et al., *Ultrapotent human antibodies protect against SARS-CoV-2 challenge via multiple mechanisms.* Science, 2020. **370**(6519): p. 950-957.
14. Wrapp, D., et al., *Cryo-EM structure of the 2019-nCoV spike in the prefusion conformation.* Science, 2020. **367**(6483): p. 1260-1263.
15. Roberts, A., et al., *A Recent Update on Advanced Molecular Diagnostic Techniques for COVID-19 Pandemic: An Overview.* Front Immunol, 2021. **12**: p. 732756.
16. Du, L., et al., *The spike protein of SARS-CoV--a target for vaccine and therapeutic development.* Nat Rev Microbiol, 2009. **7**(3): p. 226-36.
17. Piccoli, L., et al., *Mapping Neutralizing and Immunodominant Sites on the SARS-CoV-2 Spike Receptor-Binding Domain by Structure-Guided High-Resolution Serology.* Cell, 2020. **183**(4): p. 1024-1042 e21.
18. Shrock, E., et al., *Viral epitope profiling of COVID-19 patients reveals cross-reactivity and correlates of severity.* Science, 2020. **370**(6520).
19. Zhao, J., et al., *COVID-19: Coronavirus Vaccine Development Updates.* Front Immunol, 2020. **11**: p. 602256.
20. FDA. *Emergency Use Authorization 108*. https://www.fda.gov/media/155053/download 2021.
21. FDA. *Emergency Use Authorization 105*. 2021.
22. Parums, D.V., *Editorial: Current Status of Oral Antiviral Drug Treatments for SARS-CoV-2 Infection in Non-Hospitalized Patients.* Med Sci Monit, 2022. **28**: p. e935952.

23. Sreerama, N. and R.W. Woody, *Estimation of protein secondary structure from circular dichroism spectra: comparison of CONTIN, SELCON, and CDSSTR methods with an expanded reference set.* Anal Biochem, 2000. **287**(2): p. 252-60.
24. Olugbile, S., et al., *Malaria vaccines - The long synthetic peptide approach: Technical and conceptual advancements.* Curr Opin Mol Ther, 2010. **12**(1): p. 64-76.
25. ECDC. *SARS-CoV-2 variants of concern as of 03 February 2022*. 2022 [cited (https://www.ecdc.europa.eu/en/covid-19/variants-concern.
26. Pino, P., et al., *Trimeric SARS-CoV-2 Spike Proteins Produced from CHO Cells in Bioreactors Are High-Quality Antigens.* Processes, 2020. **8**(12): p. 1539.
27. Whitmore, L. and B.A. Wallace, *DICHROWEB, an online server for protein secondary structure analyses from circular dichroism spectroscopic data.* Nucleic Acids Res, 2004. **32**(Web Server issue): p. W668-73.
28. Olugbile, S., et al., *Malaria vaccine candidate: design of a multivalent subunit alpha-helical coiled coil poly-epitope.* Vaccine, 2011. **29**(40): p. 7090-9.
29. Grifoni, A., et al., *A Sequence Homology and Bioinformatic Approach Can Predict Candidate Targets for Immune Responses to SARS-CoV-2.* Cell Host Microbe, 2020. **27**(4): p. 671-680 e2.
30. Zhou, T., et al., *Cryo-EM Structures Delineate a pH-Dependent Switch that Mediates Endosomal Positioning of SARS-CoV-2 Spike Receptor-Binding Domains.* bioRxiv, 2020.
31. Marien, J., et al., *Evaluation of a surrogate virus neutralization test for high-throughput serosurveillance of SARS-CoV-2.* J Virol Methods, 2021. **297**: p. 114228.
32. Pratesi, F., et al., *BNT162b2 mRNA SARS-CoV-2 Vaccine Elicits High Avidity and Neutralizing Antibodies in Healthcare Workers.* Vaccines (Basel), 2021. **9**(6).
33. Tan, C.W., et al., *A SARS-CoV-2 surrogate virus neutralization test based on antibody-mediated blockage of ACE2-spike protein-protein interaction.* Nat Biotechnol, 2020. **38**(9): p. 1073-1078.
34. Walls, A.C., et al., *Structure, Function, and Antigenicity of the SARS-CoV-2 Spike Glycoprotein.* Cell, 2020. **181**(2): p. 281-292 e6.
35. Sharma, O., et al., *A Review of the Progress and Challenges of Developing a Vaccine for COVID-19.* Front Immunol, 2020. **11**: p. 585354.
36. Baden, L.R., et al., *Efficacy and Safety of the mRNA-1273 SARS-CoV-2 Vaccine.* N Engl J Med, 2021. **384**(5): p. 403-416.
37. Shang, J., et al., *Structural basis of receptor recognition by SARS-CoV-2.* Nature, 2020. **581**(7807): p. 221-224.
38. Amanat, F. and F. Krammer, *SARS-CoV-2 Vaccines: Status Report.* Immunity, 2020. **52**(4): p. 583-589.
39. Kyriakidis, N.C., et al., *SARS-CoV-2 vaccines strategies: a comprehensive review of phase 3 candidates.* NPJ Vaccines, 2021. **6**(1): p. 28.
40. Silveira, M.M., G. Moreira, and M. Mendonca, *DNA vaccines against COVID-19: Perspectives and challenges.* Life Sci, 2021. **267**: p. 118919.
41. Chung, J.Y., M.N. Thone, and Y.J. Kwon, *COVID-19 vaccines: The status and perspectives in delivery points of view.* Adv Drug Deliv Rev, 2021. **170**: p. 1-25.
42. Krause, P.R., et al., *Considerations in boosting COVID-19 vaccine immune responses.* Lancet, 2021. **398**(10308): p. 1377-1380.

552

553 **Data availability**

554 Data that support the study are in the REDCap database, available from the corresponding author
555 upon reasonable request.

556 **Acknowledgments**

557 We thank the volunteers from Pisa (Italy) and from Cali (Colombia) for their invaluable
558 contribution to the study.

559 **Funding**

560 This work was funded by Colciencias (grant 529-2009), the MVDC/CIV Foundation and by the
561 Italian Ministry of Health grant *COVID-2020-12371849*

562 **Competing Interest**

563 The authors declare no competing interest.

564 **Author contributions**

565 Conceptualization: G.C., A.M.P., A.K., S.H.

566 Formal analysis: G.C., M.A.H., A.M.P, A.K., S.H.,

567 Investigation: G.C., P.R., F.P., P.M., L.P., F.E., A.C., I.P.M, S.B., D.K., M.M.D, S.Q., M.A.H., S.H.,

568 Methodology: M.A.H., F.P., F.E., S.H., G.C.,

569 Project administration: M.A.H., G.C.

570 Resources: G.C., S.H., A.K., A.M.P.

571 Supervision: M.A.H., S.H., G.C.

572 Validation: M.A.H., G.C., A.K.

573 Visualization: M.A.H., S.H., G.C.

574 Writing: P.M., P.R., G.C., S.H., A.K.,

575

576 **Co-authors Emails:**

577 Andrey V. Kajava, <andrey.kajava@crbm.cnrs.fr>

578 Anna M. Papini, <annamaria.papini@unifi.it>

579 Saidou Balam, <balamsira@yahoo.fr>

580 Drissa Konaté, <dkonate@icermali.org>

Mahamadou M Diakité, <mdiakite@icermali.org>
Paola Migliorini, <paola.migliorini@unipi.it>
Paolo Rovero, <paolo.rovero@unifi.it>
Federico Pratesi, <federico.pratesi@unipi.it>
Lorenzo Pacini, <l.pacini@unifi.it>
Fosca Errante, <fosca.errante@unifi.it>
Alfonso Carotenuto, <alfonso.carotenuto@unina.it>
Sebastian Quiceno, <squiceno@inmuno.org>
Irina Peña-Moreno, <irina.penamoreno@gmail.com>
Myriam Arévalo-Herrera, <marevalo@inmuno.org>
Giampietro Corradin, <giampietro.corradin@unil.ch>
Socrates Herrera, <sherrera@inmuno.org>

Tables and Figures

Table 1. Synthesized RBM Peptide sequences

Name	Sequence	Amino acids
$RBM_{436-507}$	Ac-WNSNNLDSKVGGNYNYLYRLRKSNLKPFERDISTEIYQAGSTPCNGVEGFNCYFPLQSYGFQPTNGVGYQP-NH_2	436-507
P11	Ac-FNSYFPLQSYGFQPTNGVGYQP-NH_2	486-507
P12	Ac-GSTPCNGVEGFNCYFPLQSY-NH_2	476-495
P13	Ac-RDISTEIYQAGSTPSNGVEG-NH_2	466-485
P14	Ac-FRKSNLKPFERDISTEIYQA-NH_2	456-475
P15	Ac-GGNYNYLYRLFRKSNLKPFE-NH_2	446-465
P16	Ac-WNSNNLDSKVGGNYNYLYRL-NH_2	436-455

Underlined sequences in peptides P3 and P12 represent disulfide bridges. Serine residues (S) highlighted in red in peptides P11 and P13 replace native Cysteines.

FIGURE LEGENDS

Figure 1.
(**A**) Atomic 3D structure of the S trimer in the prefusion conformation (27). RBD is shown in ribbon representation (dark green). Region 476-507 is in orange. (**B**) Complex between RBD (green-orange) and ACE2 receptor (light cyan) (12). (**C**) Conformation of the RBM peptide (436-507) within the RBD. Cysteine residues are shown as spheres. (**D**) Circular Dicroism of $RBM_{436-507}$ synthetic peptide used in this work.

Figure 2
Analysis of Anti-Spike (**A**), anti-RBD (**B**) and anti-$RBM_{436-507}$ (**C**) antibodies in immunized mice at 0, 20, 40 and 140 days post-immunization. SD is < 20% of the mean.

Figure 3.
Cross reactivity of anti-S (top panel), anti-RBD (middle panel) and anti-$RBM_{436-507}$ (bottom panel) from mice immunized with Spike, RBD and RBM antigens. SD is < 20% of the mean.

Figure 4.
Capture ELISA with mice anti-$RBM_{436-507}$ Ab eluted with Gly pH 2.5. Captured proteins RBM, S and RBD, developed with mouse anti-RBM and rabbit anti-mouse alkaline phosphatase conjugate.

Figure 5. **Anti-Spike and anti-RBD antibodies in Covid-19 patients.**
Distribution of anti-S IgG (**A**) and anti RBD IgG (**B**) in Covid-19 patients as compared to normal controls (NHS). Correlation of anti-S IgG and anti-RBD IgG in COVID-19 patients (**C**). $p < 0.05$ was considered significant.

Figure 6. Anti-$RBM_{436-507}$ antibodies in Covid-19 patients.
Distribution of anti RBM IgG (**A**), IgM (**B**) and IgA (**C**) in Covid-19 patients is shown compared to normal controls (NHS). Correlation of anti-RBM IgG with anti-Spike (**D**) or anti-RBD (**E**) IgG in COVID-19 patients (**D**). Distribution of anti-RBM antibody isotypes (**F**). $p < 0.05$ was considered significant.

Figure 7. Neutralizing ability of antibodies in mice.
Neutralizing ability of anti-Spike, anti-RBD and anti-RBM antibodies from immunized mice. Results are shown as the percentage of inhibition of specific antibodies at different days (0, 40, and 115) post-immunization.
Figure 8. Fine specificity of anti-RBM436-507 antibodies in Covid-19 patients.

Reactivity of Anti-RBM positive Covid-19 sera with 20-mers overlapping peptides (P11-P16) covering the entire $RBM_{436-507}$ sequence. Results are shown as percentage of anti-RBM positive sera reacting with the specific peptide.

Figure 9. Neutralizing ability of antibodies in Covid-19 patients

Neutralizing ability of antigen eluted anti-Spike, anti-RBD and anti-RBM antibodies in Covid-19 patients. Results are shown as the percentage of inhibition of ACE-HRP binding to RBD.

Figure Supp 1

a. Humoral response induced in mice after immunization of sera diluted at 1:100. Antibody titers are expressed as O.D. of samples taken at days 0, 20, 40 and 140.

b. Titration of mice sera from day 140 tested by ELISA, using three-fold serial dilutions of sera, starting at 1:100. Antibody titers are expressed as O.D.

Figure Supp 2

Distribution of Anti-Spike antibodies (2A) and anti-RBD antibodies (2B) analyzed by ELISA under acid conditions (pH 5)

FIGURES

Figure 1

Here use A, B, C, and D (capitals, as done for the other figs) and A should be on top left

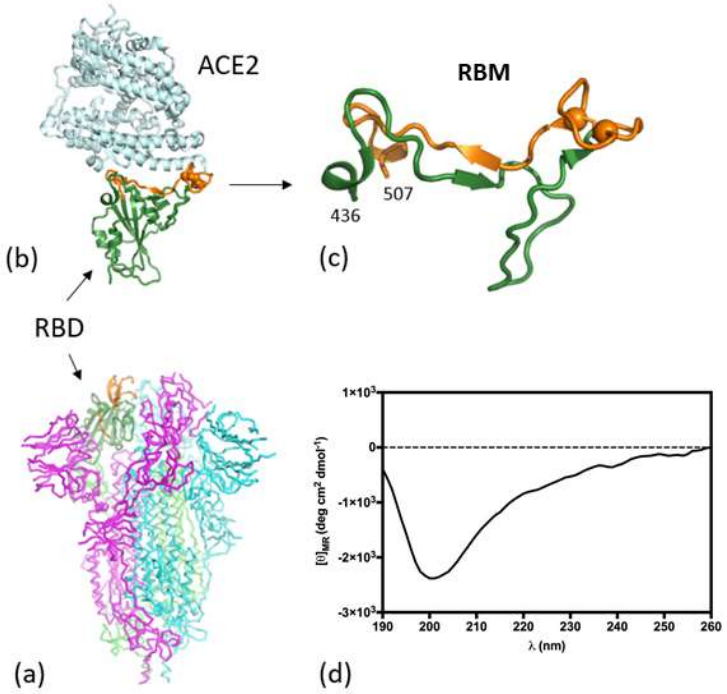

Figure 2

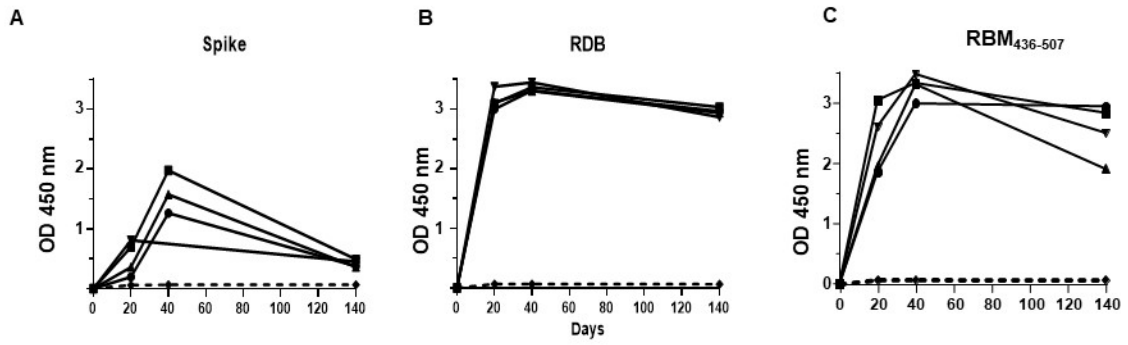
A
Spike
OD 450 nm
0
1
2
3
0 20 40 60 80 100 120 140
B
RDB
OD 450 nm
0
1
2
3
0 20 40 60 80 100 120 140
Days
C
RBM436-507
OD 450 nm
0
1
2
3
0 20 40 60 80 100 120 140

Figure 3

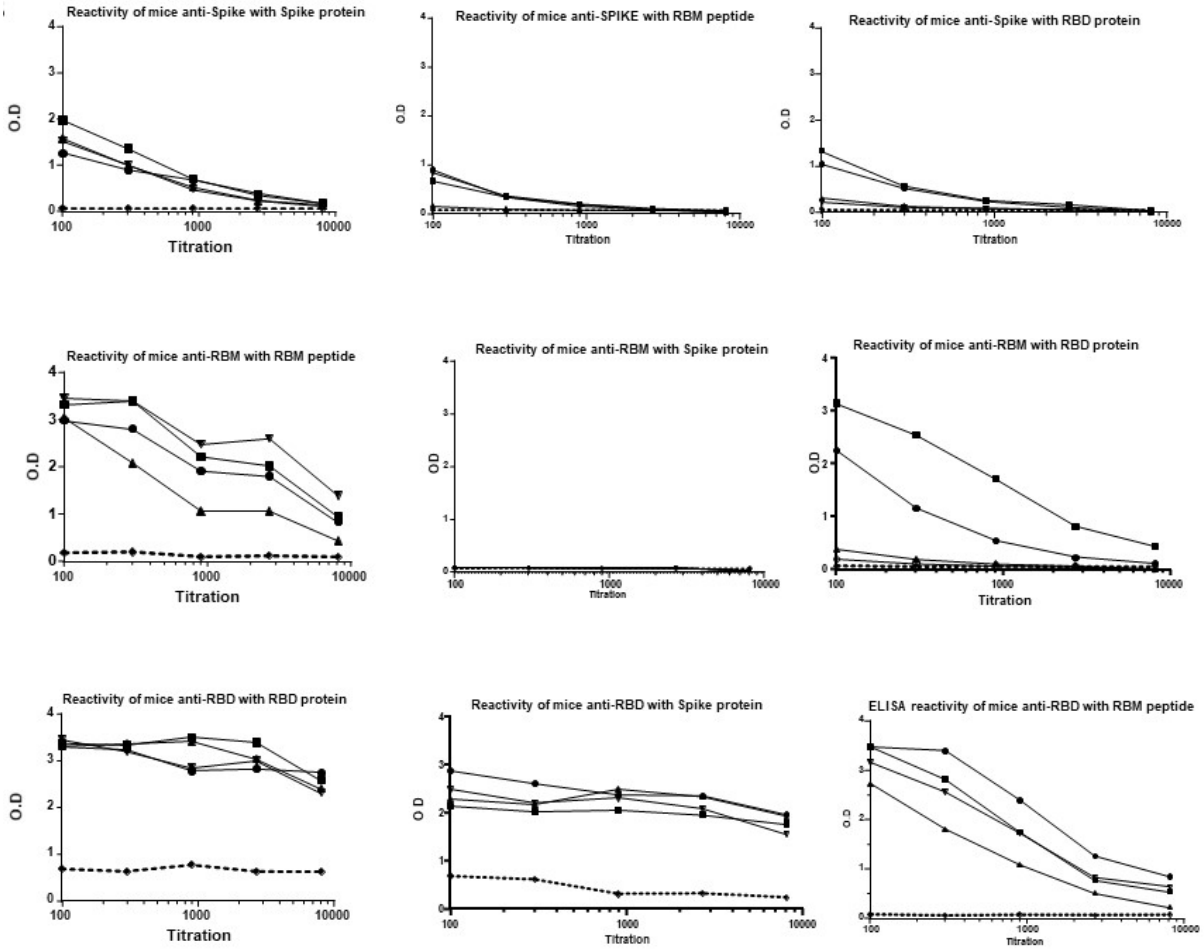
Reactivity of mice anti-Spike with Spike protein
Reactivity of mice anti-SPIKE with RBM peptide
Reactivity of mice anti-Spike with RBD protein
Reactivity of mice anti-RBM with RBM peptide
Reactivity of mice anti-RBM with Spike protein
Reactivity of mice anti-RBM with RBD protein
Reactivity of mice anti-RBD with RBD protein
Reactivity of mice anti-RBD with Spike protein
ELISA reactivity of mice anti-RBD with RBM peptide
O.D
Titration

Figure 4

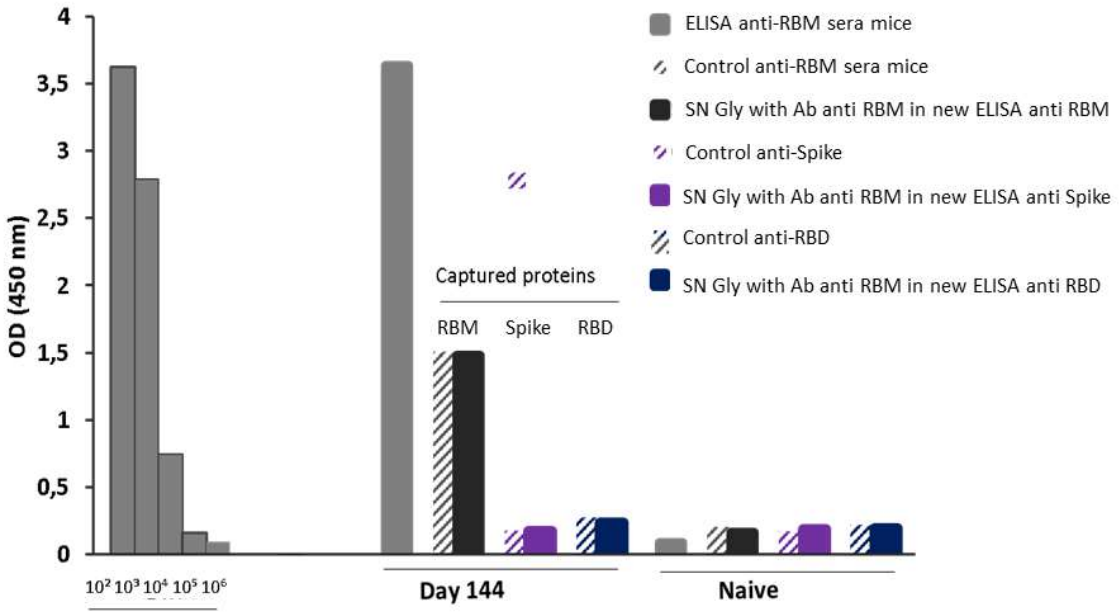
OD (450 nm)
4
3,5
3
2,5
2
1,5
1
0,5
0
ELISA anti-RBM sera mice
Control anti-RBM sera mice
SN Gly with Ab anti RBM in new ELISA anti RBM
Control anti-Spike
SN Gly with Ab anti RBM in new ELISA anti Spike
Control anti-RBD
SN Gly with Ab anti RBM in new ELISA anti RBD
Captured proteins
RBM
Spike
RBD
10^2 10^3 10^4 10^5 10^6
Day 144
Naive

Figure 5

Figure 6

Here eliminate the “6” below from panels, just show A, B, C etc- as you show in Fig. 2 above

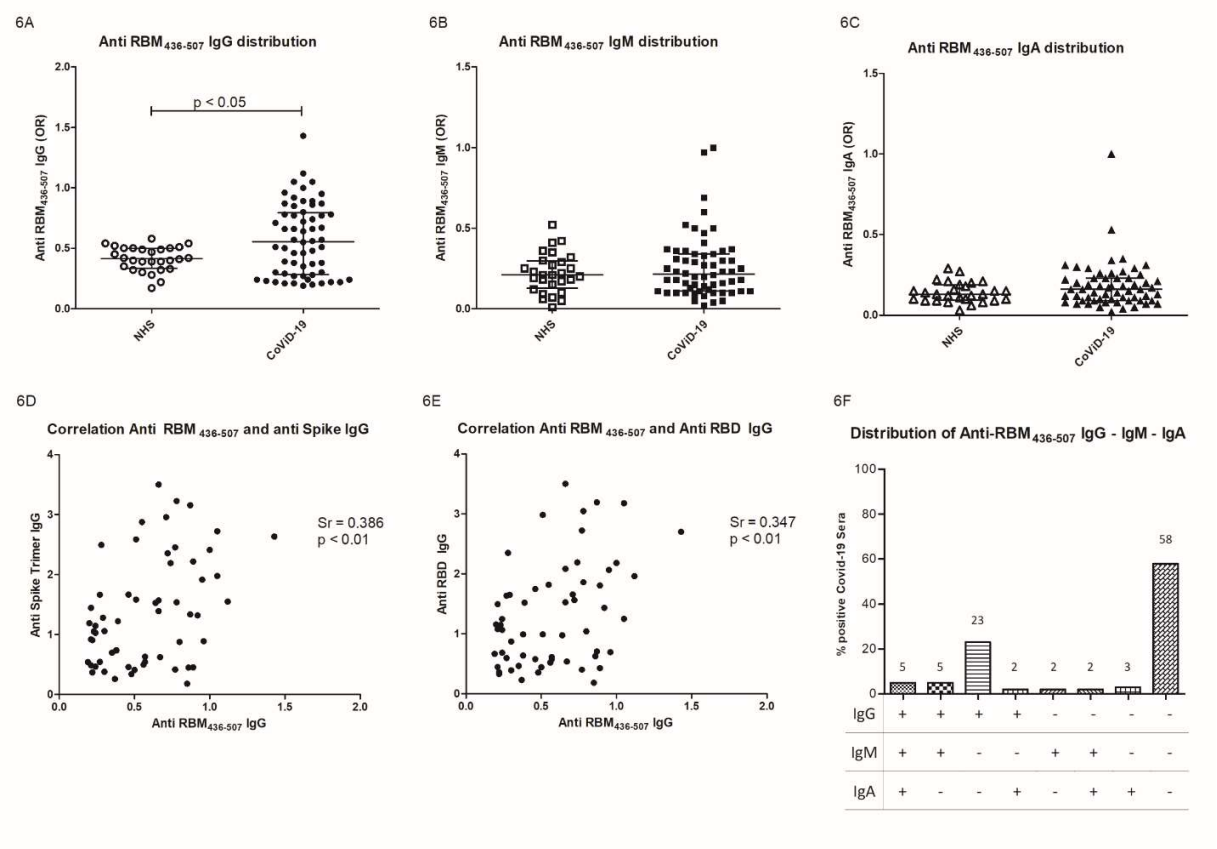

Figure 7

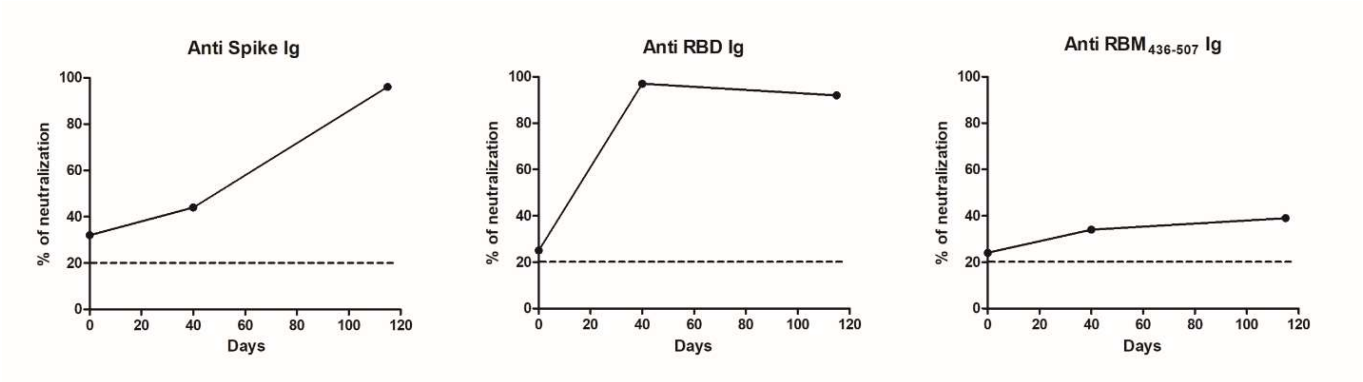
Anti Spike Ig
% of neutralization
Days
Anti RBD Ig
% of neutralization
Days
Anti RBM436-507 Ig
% of neutralization
Days

Figure 8

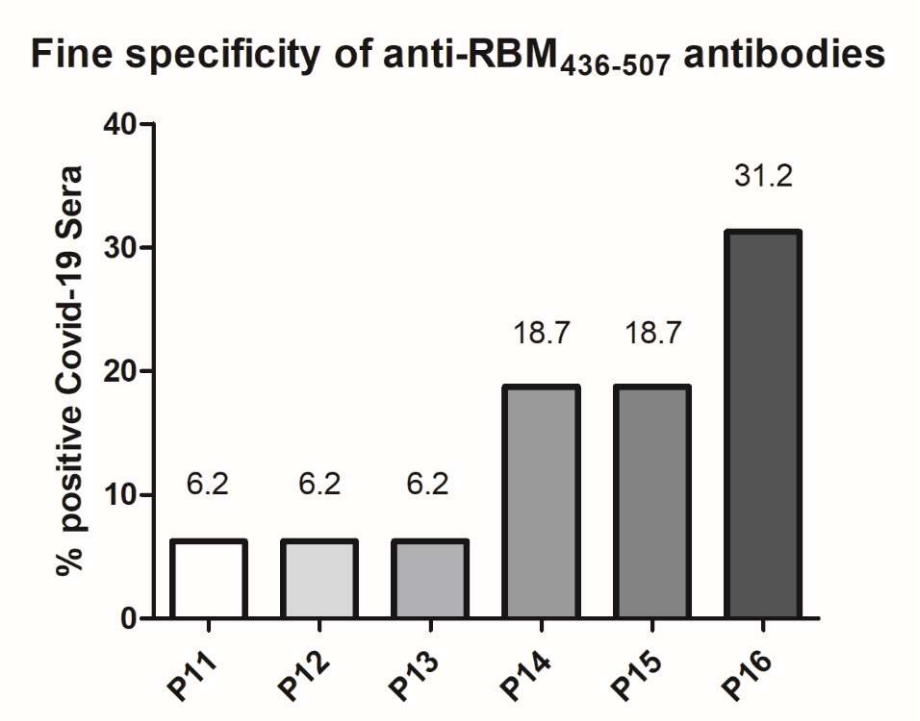
Fine specificity of anti-RBM436-507 antibodies
% positive Covid-19 Sera
40
30
20
10
0
6.2
6.2
6.2
18.7
18.7
31.2
P11
P12
P13
P14
P15
P16

Figure 9

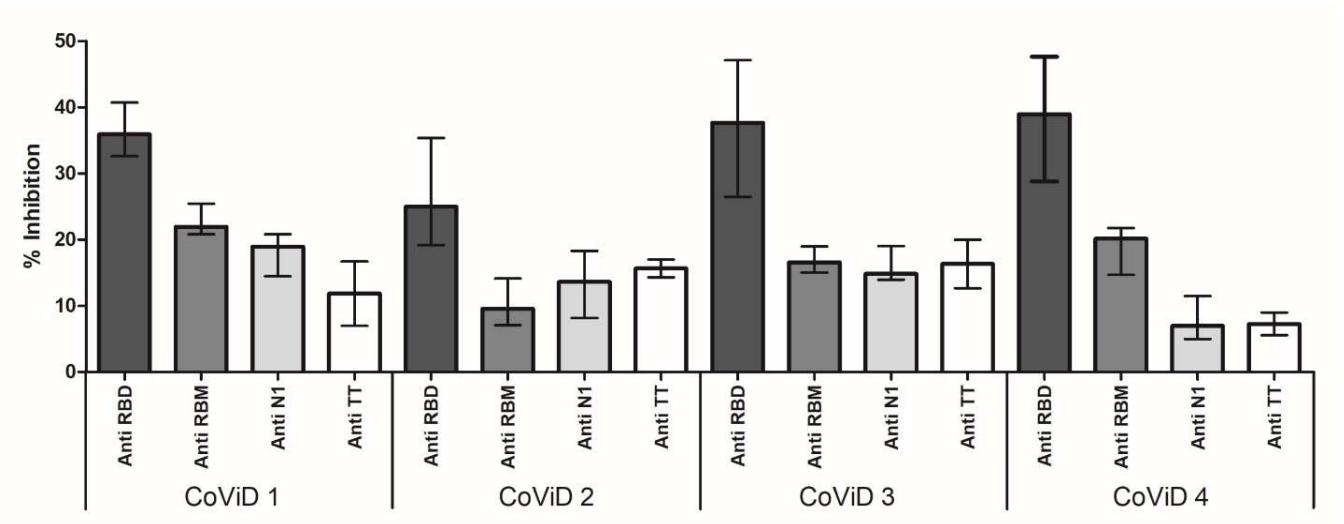
% Inhibition
50
40
30
20
10
0
Anti RBD
Anti RBM
Anti N1
Anti TT
CoViD 1
CoViD 2
CoViD 3
CoViD 4

Supplem. Fig 1

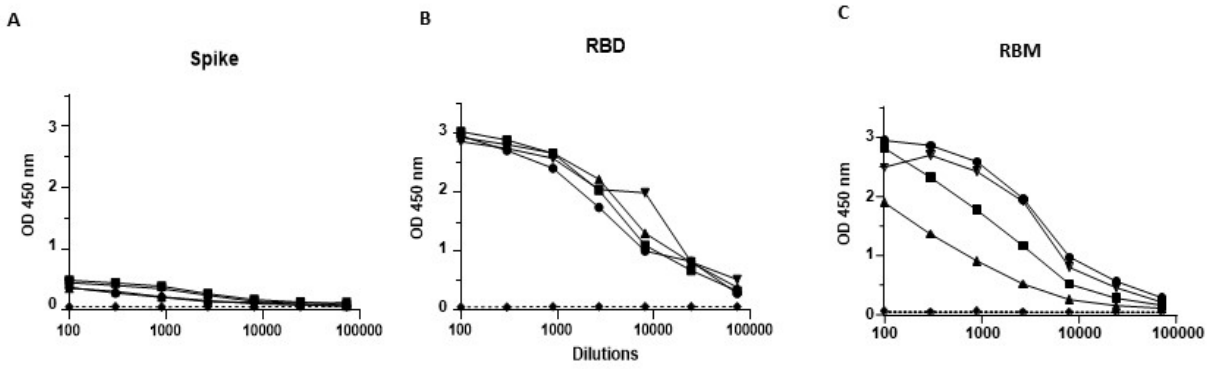

Supplem. Fig 2

A

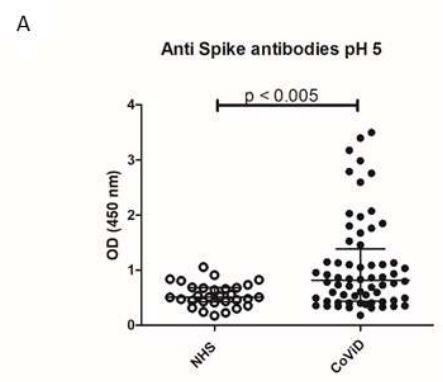

B